Cell

Reprogramming of the Circadian Clock by Nutritional Challenge

Kristin L. Eckel-Mahan,[1] Vishal R. Patel,[2] Sara de Mateo,[1] Ricardo Orozco-Solis,[1] Nicholas J. Ceglia,[2] Saurabh Sahar,[1] Sherry A. Dilag-Penilla,[1] Kenneth A. Dyar,[3] Pierre Baldi,[2] and Paolo Sassone-Corsi[1,*]
[1]Center for Epigenetics and Metabolism, Department of Biological Chemistry, University of California, Irvine, Irvine, CA 92697, USA
[2]Institute for Genomics and Bioinformatics, School of Information and Computer Sciences, University of California, Irvine, Irvine, CA 92697, USA
[3]Venetian Institute of Molecular Medicine, Padova 35129, Italy
*Correspondence: psc@uci.edu
http://dx.doi.org/10.1016/j.cell.2013.11.034

SUMMARY

Circadian rhythms and cellular metabolism are intimately linked. Here, we reveal that a high-fat diet (HFD) generates a profound reorganization of specific metabolic pathways, leading to widespread remodeling of the liver clock. Strikingly, in addition to disrupting the normal circadian cycle, HFD causes an unexpectedly large-scale genesis of de novo oscillating transcripts, resulting in reorganization of the coordinated oscillations between coherent transcripts and metabolites. The mechanisms underlying this reprogramming involve both the impairment of CLOCK:BMAL1 chromatin recruitment and a pronounced cyclic activation of surrogate pathways through the transcriptional regulator PPARγ. Finally, we demonstrate that it is specifically the nutritional challenge, and not the development of obesity, that causes the reprogramming of the clock and that the effects of the diet on the clock are reversible.

INTRODUCTION

A large number of physiological events follow circadian rhythmicity. Examples of biological circadian rhythms include sleeping, eating, hormone and neurotransmitter secretion, and even proficiency at cognitive tasks (Dibner et al., 2010; Gerstner et al., 2009; Menet and Rosbash, 2011; Sahar and Sassone-Corsi, 2012). At the cellular level, these rhythms are controlled by transcriptional feedback loops that produce oscillations in gene expression, a process associated with circadian changes in chromatin architecture, messenger RNA (mRNA) processing, protein activity, and protein turnover (Feng and Lazar, 2012; Koike et al., 2012; Morf et al., 2012; Yoo et al., 2013; Masri et al., 2013; Rey et al., 2011). Rhythmicity in transcription is controlled in large part by specialized factors, including CLOCK, BMAL1, PERs, CRYs, and others (Ko and Takahashi, 2006; O'Neill et al., 2008). Coordination at the cellular level is necessary for tissue-specific oscillations that control circadian physiology (Bray and Young, 2009; Hastings et al., 2008; Schibler and Sassone-Corsi, 2002; Zhang et al., 2010). Accumulating evidence supports the notion that oscillating metabolites are also important for the maintenance of cellular rhythmicity (Eckel-Mahan et al., 2012; Nakahata et al., 2009; O'Neill et al., 2011; Dallmann et al., 2012; Ramsey et al., 2009), but the extent to which the circadian metabolome is affected by nutritional stress is not known.

Metabolic homeostasis is not maintained when components of the circadian clock are missing or functioning improperly (Kondratov et al., 2006; Lee et al., 2011; Marcheva et al., 2010; Rudic et al., 2004; Sadacca et al., 2011; Shi et al., 2013; Turek et al., 2005; Zhang et al., 2010), and circadian disruption can result in disorders such as diabetes, obesity, and cardiac disease (Antunes et al., 2010; Doi et al., 2010; Drake et al., 2004; Fonken et al., 2010; Froy, 2010; Knutsson, 2003; Lamia et al., 2008; Sharifian et al., 2005; Suwazono et al., 2008). Conversely, metabolic disruptions such as the restriction of energy intake to a phase that opposes that of the traditional feeding phase, can reset some peripheral clocks almost entirely, disrupting energy balance (Arble et al., 2009; Damiola et al., 2000; Hughes et al., 2009; Stokkan et al., 2001; Vollmers et al., 2009). Hepatic circadian rhythmicity, in particular, is highly responsive to cyclic energy intake (Hatori et al., 2012; Pendergast et al., 2013; Vollmers et al., 2009).

The molecular mechanisms by which a high-fat diet (HFD) affects the circadian clock are not known. Using high-throughput profiling of the liver metabolome and transcriptome, we establish that HFD has multifaceted effects on the clock, including a phase advance of metabolite and transcript oscillations that are maintained on the diet, as well as an abolition of otherwise oscillating transcripts and metabolites. In addition to these disruptive effects, we find a surprising, elaborate induction of newly oscillating transcripts and metabolites. Thus, HFD has pleiotropic effects that lead to a reprogramming of the metabolic and transcriptional liver pathways. These are mediated both by interfering with CLOCK:BMAL1 recruitment to chromatin and by inducing the de novo oscillation of PPARγ-mediated transcriptional control at otherwise noncyclic genes.

RESULTS

Extensive and Specific Reorganization of the Circadian Metabolome by HFD

To understand how altered nutrients affect circadian metabolism, we explored the effect of HFD in mice by studying the

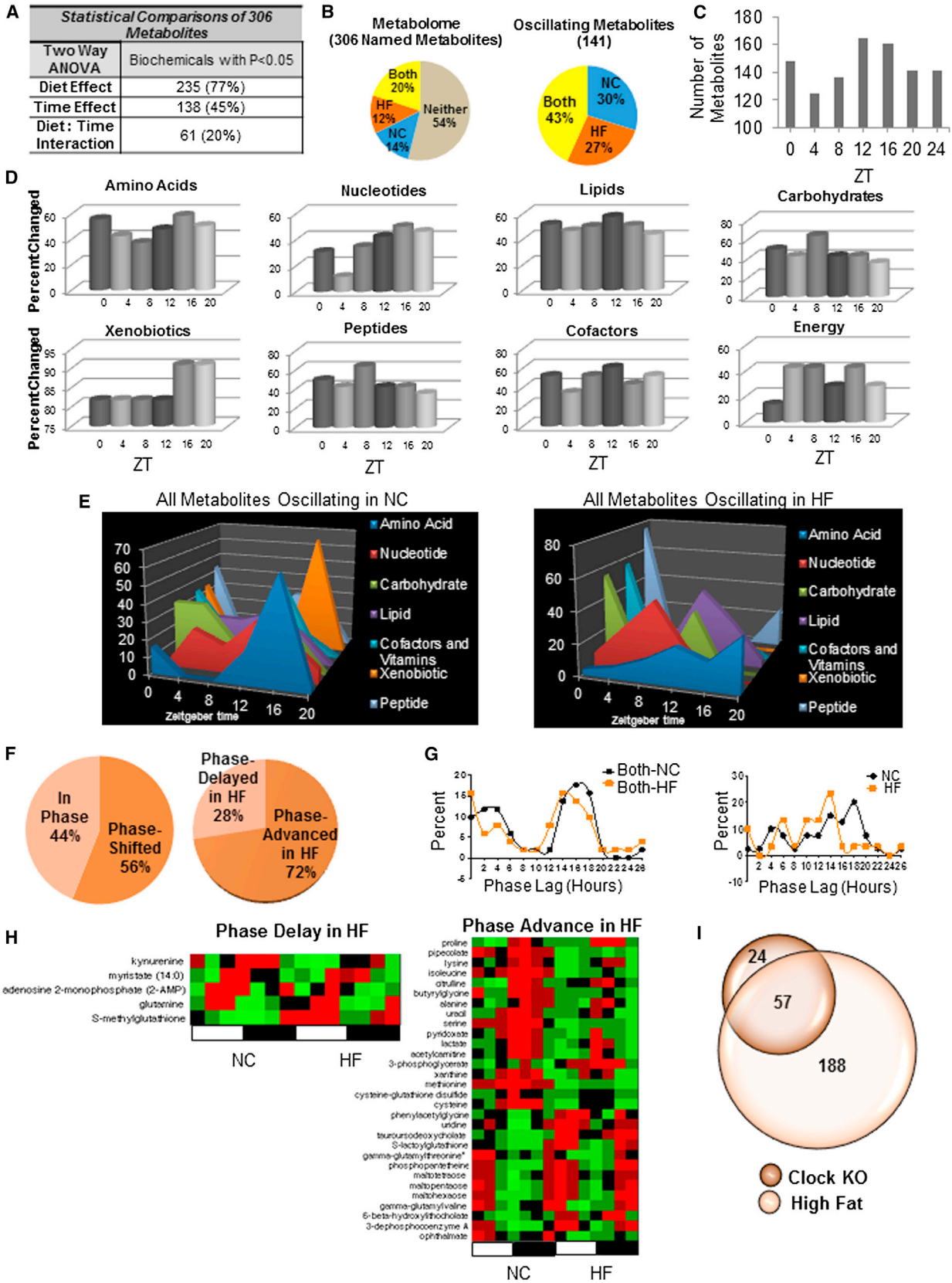

(legend on next page)

hepatic metabolome, where a large number of metabolites are circadian or clock controlled (Dallmann et al., 2012; Eckel-Mahan et al., 2012; Kasukawa et al., 2012). After 10 weeks on a HFD, mice displayed expected metabolic features (Figure S1 available online). Importantly, the timing and quantity of energy intake was similar between feeding groups (Figure S1 and Extended Experimental Procedures). Metabolome profiles were obtained by tandem mass spectrometry (MS/MS) and gas chromatography-mass spectrometry (GC/MS) from livers isolated every 4 hr throughout the circadian cycle (Evans et al., 2009). A large number of metabolites across several metabolic pathways displayed changes in HFD-fed animals (Figure S2). Of 306 identifiable metabolites, 77% showed a diet effect, and 45% showed a time effect (Figures 1A and S2). When analyzed for circadian oscillations, 141 metabolites cycled in abundance. Of these, 61 metabolites (43%) oscillated in both feeding conditions (both), whereas 42 metabolites (30%) oscillated only in normal chow-fed animals (NC). Importantly, 38 metabolites oscillated only in HFD-fed animals (HF) (Figure 1B). Many of the metabolite changes were present at ZT12 and ZT16 (Figure 1C) and included numerous nucleotide, amino acid, and xenobiotic metabolites (Figures 1D and S2). The metabolite peak profiles differed across several of the metabolic pathways throughout the circadian cycle (Figures 1E and S2). Interestingly, the phase and amplitude of remaining oscillatory metabolites also differed. Specifically, metabolites that oscillated in both feeding conditions generally showed a shift in phase when in HFD (Figure 1F). Of the phase-shifted metabolites, 28% were delayed in phase, whereas 72% were phase-advanced in HFD (Figures 1F–1H). Considering the phase of metabolites that oscillated only in NC or only in HFD, metabolites that oscillated only in HFD tended to peak earlier (Figure 1G).

A majority of metabolite oscillations previously shown to be CLOCK dependent (Eckel-Mahan et al., 2012) are affected by HFD (Figure 1I). As seen in our previous experiments, specific metabolic subpathways are circadian. For example, lysine metabolism is highly rhythmic in normal feeding conditions (Eckel-Mahan et al., 2012). In this study, lysine metabolism was highly rhythmic in both feeding conditions. Specifically, glutarate, lysine, 2-aminoadipate, and pipecolate showed oscillatory abundance in both conditions (Table S1 and http://circadiomics.igb.uci.edu/). On the other hand, pyrimidine metabolism displayed rhythmicity only under NC condition. For example, cytidine 5′-monophosphate (5-CMP), 2′-deoxycytidine, and 2′-deoxycytidine 5′-monophosphate all lost oscillation in HFD. (Table S1 and http://circadiomics.igb.uci.edu/).

Strikingly, HFD completely blocked oscillation of nicotinamide adenine dinucleotide (NAD^+) (Table S1 and Figure 4A). A previous report demonstrated reduced hepatic NAD^+ under HFD (Yoshino et al., 2011). Thus, HFD may modulate its negative influence on energy balance by eliminating circadian oscillations in NAD^+ rather than inducing a static decrease in total NAD^+ content. The lack of circadian NAD^+ accumulation under HFD supports the observation that NAD^+ is high during fasting (Rodgers et al., 2005). Animals fed a HFD may never achieve such an energy-depleted state due to the constant and nonoscillatory levels of glucose. The molecular mechanism leading to the impairment in NAD^+ oscillation in HFD constitutes a paradigm of clock transcriptional reprogramming through the control of the *Nampt* gene (Figures 3B and 4E).

A large number of lipid metabolites were affected by HFD (Figure S2). Coenzyme A, a cofactor involved in fatty acid synthesis and β oxidation, displayed a circadian profile in HFD that was substantially increased in amplitude, as did its precursors phosphopantothein and 3-dephosphocoenzyme A. Many amino acid metabolites continued to oscillate in both conditions, even though their relative abundance was substantially reduced by the HFD, likely due to increased gluconeogenesis. We conclude that the HFD impinges on the circadian metabolome in three possible manners: ablation, phase advancement, or promotion of oscillation for specific metabolites.

Reprogramming the Circadian Transcriptome

We analyzed the circadian transcriptome using the same liver samples used for the metabolome. In all, 2,828 transcripts oscillated in expression; of these, 49.5% (1,394) were rhythmic only in the NC condition (Figure 2A). An additional 778 were rhythmic in both NC and HF conditions, and a surprising 654 were newly oscillating exclusively in HFD (Figures 2A and 2B). When analyzed for singular enrichment in metabolic pathways, we found that genes oscillating in both NC and HF showed unique annotations, including purine metabolism and circadian rhythm (Figure 2C). The persistence of circadian clock gene oscillation in both NC and HFD validates the notion that circadian oscillation within the core clock genes is highly resistant to perturbation, whereas clock output genes are more sensitive to food as a zeitgeber (Damiola et al., 2000). Metabolic pathways whose oscillation was uniquely lost in HFD included ubiquitin-mediated proteolysis and insulin signaling (Figure 2E).

Figure 1. A HDF Alters the Circadian Profile of the Metabolome

(A) Number of hepatic metabolites affected by diet or time.

(B) The hepatic circadian metabolome consists of metabolites that oscillate in both groups of animals regardless of diet (Both), metabolites that oscillate only in animals fed normal chow (NC), and metabolites that oscillate only in animals fed HFD (HF). $p < 0.05$, JTK_cycle, and $n = 5$ biological replicates.

(C) The number of hepatic metabolites altered by the HFD at each zeitgeber time (ZT).

(D) Percent of metabolites in a metabolic pathway changing at a specific ZT in HF animals.

(E) Metabolic landscapes depict the percent of oscillatory metabolites that peak at a specific ZT for each feeding condition compared to the total number of oscillatory metabolites in that metabolic pathway.

(F) Proportion of metabolites that oscillate on both diets that are in phase or phase shifted (left) and the direction of the phase shift (right).

(G) Phase graph of metabolites that oscillate in both conditions (left) or only in the NC or HF conditions (right).

(H) Heat maps depicting phase-delayed or phase-advanced metabolites in HF livers.

(I) Overlap of metabolites that are both CLOCK dependent and sensitive to a HF diet.

See also Figures S1 and S2 and Table S1.

A

Total number of oscillatory transcripts: 2826	
Group	Oscillatory Transcripts, $P<0.01$
NC only	1394
Both NC and HF	778
HF only	654

B

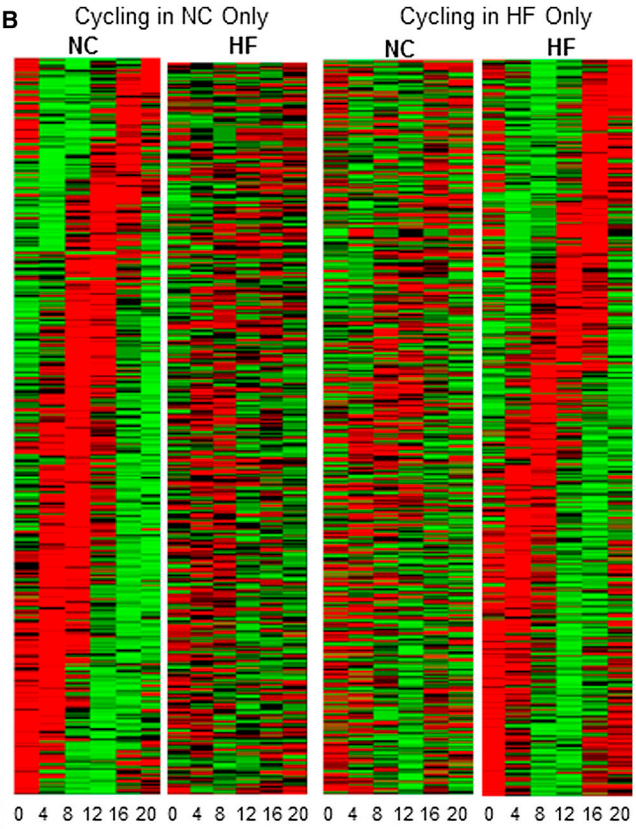

C

Oscillating in Both (778)

KEGG Pathway	
Pathways in Cancer	20
Protein Processing in Endoplasmic Reticulum	16
Purine Metabolism	15
Measles	14
Toxoplasmosis	14
Neurotrophin Signaling Pathway	14
Osteoclast Differentiation	13
Circadian Rhythm	13
Bile Secretion	9
Nicotinate and Nicotinamide Metabolism	6

D

Oscillating in NC only (1394)

KEGG Pathway	
Endocytosis	21
Lysosome	19
Ubiquitin Mediated Proteolysis	18
Insulin Signaling Pathway	17
Hepatitis C	16
Peroxisome	12
Chronic Myeloid Leukemia	12
Sphingolipid Metabolism	11
Primary Bile Acid Biosynthesis	6
Fatty Acid Biosynthesis	4

E

Oscillating in HF only (654)

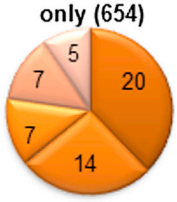

KEGG Pathway	
Protein Processing in Endoplasmic Reticulum	20
Pathways in Cancer	14
Glycerophospholipid Metabolism	7
Antigen Processing and Presentation	7
N-Glycan Biosynthesis	5

F

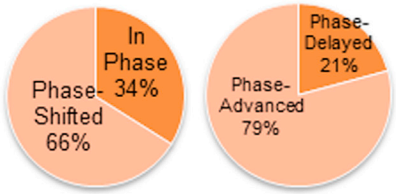

G

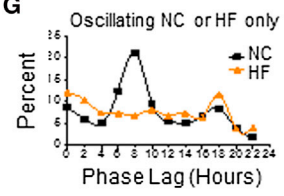

H

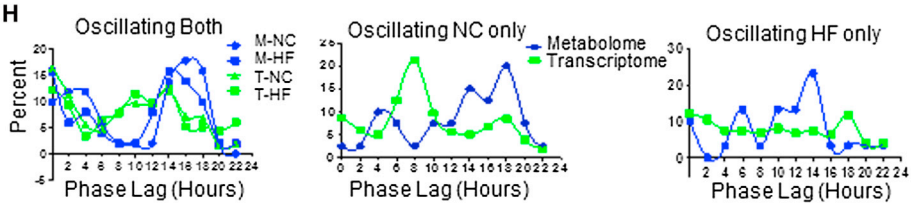

I

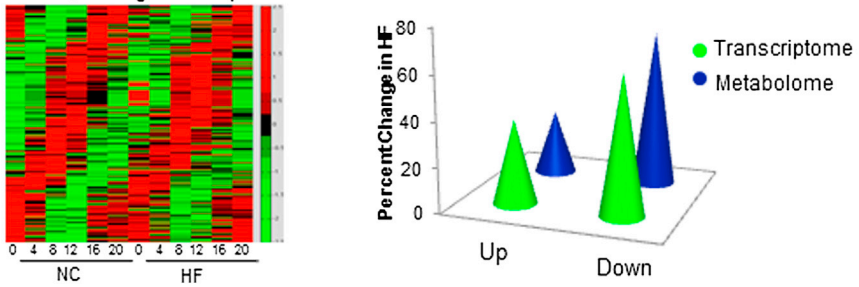

(legend on next page)

The 654 transcripts that gained rhythmicity exclusively in HFD attracted our attention. Only five annotation groups were found, with glycerophospholipid metabolism, antigen processing and presentation, and N-glycan biosynthesis as the uniquely oscillating pathways. Three members of the oligosaccharyltransferase complex (OSTC) were among this newly oscillating group, including a subunit of the oligosaccharyltransferase complex homolog A, *Ostc*. Importantly, specific N-glycans have been observed to be substantially elevated in the serum of *db/db* mice and in the serum of human subjects with type 2 diabetes (Itoh et al., 2007). Increased expression of glycan biosynthesis genes has also been observed in serum from humans with type 2 diabetes (Das and Rao, 2007).

As 27.6% of all rhythmic genes oscillated in both NC and HF conditions, we analyzed their phase of expression. Of these 778 genes, 34% oscillated in phase, whereas 66% were phase shifted by HFD (Figure 2F). Remarkably, most of the oscillatory transcripts in this category showed a phase profile that was, as for the metabolome, phase advanced in HFD. Only 21% showed a phase delay, whereas 79% of the shifted transcripts showed a phase advance (Figure 2F). Analysis of the phase of transcripts that oscillated only in NC or HFD revealed starkly different profiles. Specifically, oscillatory transcripts in the NC-only group showed robust peaks between ZT4 and ZT12, whereas the HFD group showed rather an irregular phase pattern (Figure 2G). The peak of oscillatory transcripts in the NC-only condition is consistent with when the CLOCK:BMAL1 heterodimer is most active and recruited to circadian contacts (Hatanaka et al., 2010; Kondratov et al., 2003; Rey et al., 2011). When comparing the phase of the transcripts and metabolites that oscillated in both liver sets (Figure 2H, left), similar organization was seen, with transcripts and metabolites showing a biphasic pattern and transcript peaks slightly preceding metabolite peaks. Metabolite and transcript oscillations that were lost in HFD (i.e., oscillating in NC only) also showed a temporal organization with transcripts peaking prior to the majority of metabolites (Figure 2H, middle). However, coherence was not complete in HFD, with most metabolites peaking at ZT14, and transcripts remaining largely unsynchronized in phase (Figure 2H, right).

In addition to phase analysis, we studied the oscillation amplitude of both transcripts and metabolites (Figure 2I). Of all common oscillators, 62% of the 778 transcripts showed a reduction in amplitude in HFD, whereas 38% showed an increase. Similarly, 71% of metabolites showed a reduction in amplitude in HFD, whereas 29% showed an increase. We conclude that the percentage of the circadian metabolome and transcriptome are similarly affected in amplitude by HFD, stressing the coherence between these two groups of oscillators.

Coherence of Metabolome and Transcriptome

We determined the relationship within metabolic pathways between the transcriptome (of the enzymes) and the metabolome on different diets by integrating the data into the bioinformatics resource, CircadiOmics (Patel et al., 2012). We classified and grouped metabolite-enzyme edges based on the presence or absence of oscillation, as well as additional characteristics of the oscillation—specifically, the phase and amplitude (Figure 3A). The most common edge characterization (87 of 384 edges, 23%) revealed that the loss of oscillation for a particular metabolite usually was accompanied by a loss of oscillation for its related transcripts (Figures 3A and 3B). Interestingly, the second most common edge classification involved the loss of oscillatory transcript abundance in HFD but an increase in the amplitude of oscillation in the related metabolite. No phase delay in the transcriptome or metabolome was observed within the top ten edge classification scenarios, suggesting again that a significant effect of HFD is to phase advance the remaining oscillatory metabolites. Edge classification reinforced the notion that one of the effects of HFD is to reorganize the temporal coherence between the metabolome and transcriptome. The most common relationships between related transcripts and metabolites involved an opposing state of oscillation in animals fed HFD (Figures 3A and 3B).

A paradigmatic example of a metabolite whose loss of oscillation by HFD is accompanied by a dampened oscillation for its related transcript is NAD^+. Circadian NAD^+ synthesis depends on the transcriptional control by the clock of *Nampt* gene expression (Nakahata et al., 2009; Ramsey et al., 2009). HFD induces a loss of NAD^+ oscillation that parallels a dampening of *Nampt* cyclic transcription (Figures 3B, 4E, and 4F). Additional case scenarios include ornithine decarboxylase 1 (*Odc1*) and ornithine (where a concomitant loss of oscillation occurs in HFD), acyl-CoA synthetase short-chain family member 2 (*Acss2*) and coenzyme A (where loss of oscillatory transcript in HFD corresponds to an increased metabolite amplitude), and cytochrome P450 monooxygenase (*Cyp2a5*) and arachidonate (where a phase advance in transcript in HFD corresponds to a lack of oscillation in its related metabolite) (Figure 3B).

Importantly, several metabolite and transcript edges within individual pathways mirror each other in HFD-induced gain of oscillation. Remarkable examples are within the amino acid subpathway of cysteine, methionine, S-adenosylmethionine (SAM), and taurine metabolism. Indeed, both SAM and S-adenosylhomocysteine (SAH) showed newly oscillating profiles in HFD

Figure 2. The Circadian Transcriptome Is Reprogrammed by a HFD

(A) The number of oscillatory transcripts only in NC, only in HF, or in both NC and HF groups ($p < 0.01$, JTK_cycle).
(B) Heat maps for NC- and HF-only oscillating transcripts ($p < 0.05$).
(C) Gene annotation on oscillating genes with a $p < 0.01$ reveals pathways that are oscillatory in both NC and HF livers (unique pathways in bold font).
(D) Pathways in which oscillatory expression is lost by the HF diet.
(E) KEGG pathways represented by genes oscillatory only in the HF liver.
(F) Proportion of the oscillatory transcriptome shared in both liver sets that is phase shifted (left) and the direction of the phase shift (right).
(G) Phase analysis of transcripts that oscillate only in NC or HF.
(H) Circadian fluctuations of the metabolome relative to the transcriptome in both (left), NC-only (middle), or HF-only categories (right).
(I) Extent of amplitude changes in transcript abundance (heat map and graph) and metabolites (graph) after HF feeding.
See also Tables S2 and S3.

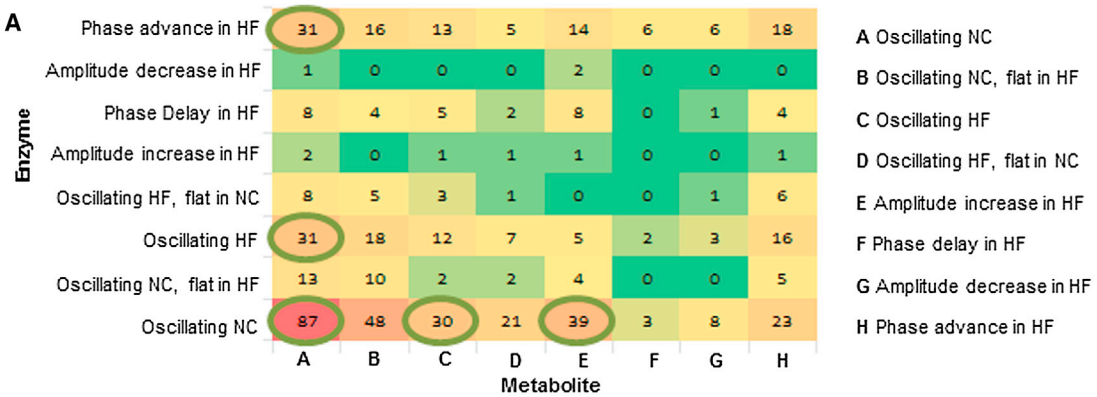

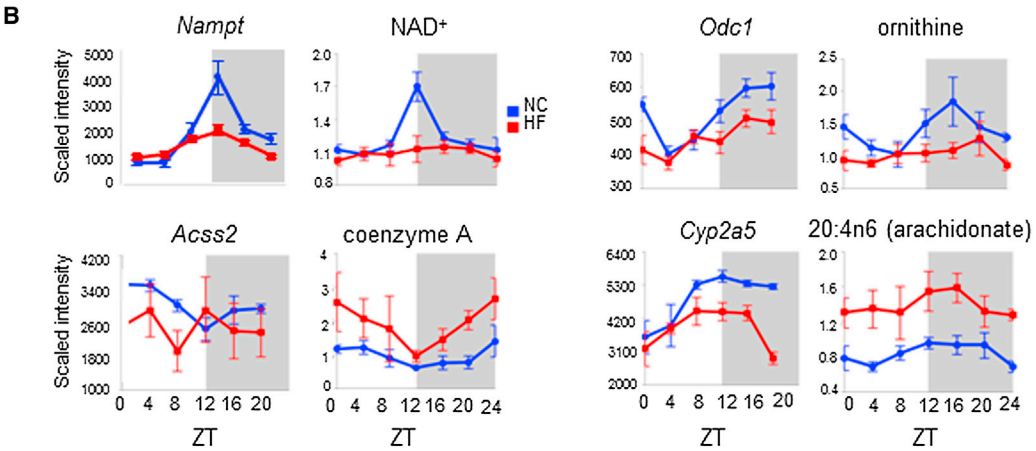

C

HFD Oscillating Metabolites	Related and HFD Oscillatory Transcripts
S-adenosylmethionine (SAM) and S-adenosylhomocysteine (SAH)	***Ehmt2***-histone methyltransferase
	Trmt2b-tRNA methyltransferase
	Ahcyl2-enzyme responsible for the conversion of SAH to adenosine and homocysteine
	Whsc1-probable histone methyltransferase
	Dph5-SAM-dependent methyltransferase

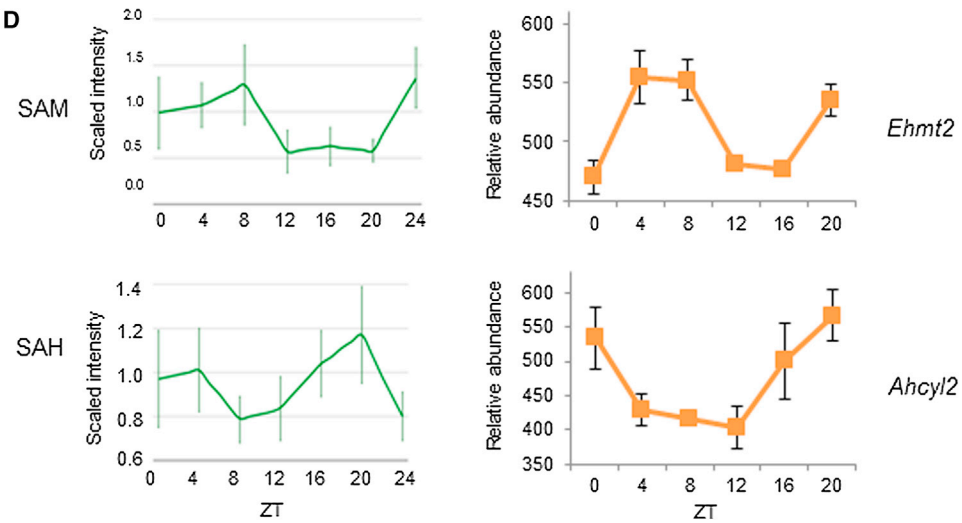

(legend on next page)

(Figure 3C). HFD-induced cycling of these metabolites was accompanied by de novo oscillation of several related enzymes, including *Ehmt*, *Trmt2b*, *Whsc1*, and *Dph5*—genes whose products have known or predicted methyltransferase activity. A relevant case is *Ahcyl2*, the gene encoding the enzyme that catalyzes the reversible conversion of SAH to adenosine and homocysteine and whose oscillation parallels the one of SAH in HFD (Figure 3D). Each metabolite and transcript identified in the livers of animals fed NC or HFD were integrated within the computational resource, CircadiOmics (Eckel-Mahan et al., 2012; Patel et al., 2012).

HFD Hinders CLOCK:BMAL1 Chromatin Recruitment to Target Genes

Activation by CLOCK:BMAL1 of target gene promoters has been linked to oscillations of a number of metabolites (Eckel-Mahan et al., 2012; Nakahata et al., 2009; Ramsey et al., 2009). Thus, we investigated the molecular mechanisms by which circadian oscillations are disrupted by HFD. First, we hypothesized that HFD might alter core clock gene expression. Importantly, most of the core circadian genes were rhythmic in the livers of HFD-fed mice (Figure 4A), displaying only weak shifts or slightly dampened patterns of oscillation, results that are cohesive with previously published work (Hatori et al., 2012; Kohsaka et al., 2007). *Per2* and *Bmal1* mRNA showed mild dampening and phase advancement, whereas *Clock* expression was unaffected (Table S2 and circadiomics.igb.uci.edu/).

One case scenario is represented by the gene *Dbp*, whose robust circadian oscillation was phase advanced in HFD (Figure 4A). Because *Clock* and *Bmal1* cyclic transcription is similar in HFD-fed mice (Figure 4A), we analyzed protein levels. Importantly, the levels of BMAL1 (Figure 4B) and CLOCK (Figure S3C) proteins were unaltered in livers of HFD-fed animals. Similarly, the phosphorylation profiles of BMAL1 in NC and HFD conditions were similar in different cellular fractions (Figures S3A and S3B). We next explored whether CLOCK:BMAL1 chromatin recruitment might contribute to the altered pattern of *Dbp* expression by chromatin immunoprecipitation (ChIP) (Ripperger and Schibler, 2006). Remarkably, BMAL1 and CLOCK recruitment was shifted in livers of HFD-fed mice (Figure 4C).

Interestingly, transcripts whose oscillation was lost in HFD were in large part peaking between ZT4 and ZT12 (Figure 2G), a time period that correlates with prominent CLOCK:BMAL1 recruitment to chromatin targets (Hatanaka et al., 2010; Kondratov et al., 2003; Rey et al., 2011). This parallels the dampening or abrogation of the oscillations of numerous metabolites previously shown to be CLOCK:BMAL1 regulated (Figure 4D). A remarkable example is NAD^+, whose cyclic levels become flat after HFD, paralleling the profile of *Nampt* transcription (Figures 4D and 4E). Similarly, the oscillations of the metabolites uridine and uracil, the abundance of which is dependent on the enzymatic activity of CLOCK:BMAL1-driven uridine phosphorylase 2 (*Upp2*) (Eckel-Mahan et al., 2012), were depressed in the livers of HFD-fed animals (Figure 4D). The amplitude of *Upp2* expression was considerably reduced under HFD (Figure 4E). Interestingly, we observed a substantial decrease in CLOCK and BMAL1 circadian occupancy on the *Upp2* and *Nampt* promoters in livers of animals fed a HFD (Figures 4F, 4G, and S3D). Importantly, oscillation in H3K4me3, a histone modification tightly associated with circadian transcription (Katada and Sassone-Corsi, 2010; Ripperger and Schibler, 2006), significantly decreased at the *Upp2* (Figure 4H) and *Nampt* (data not shown) promoters in HFD-fed animals. Thus, the profound effect elicited by HFD is caused by either phase-shifted or reduced recruitment of the CLOCK:BMAL1 complex to chromatin at the level of target promoters.

HFD-Induced Reprogramming of the Clock by PPARγ

The disruptive effect of HFD on CLOCK:BMAL1 chromatin recruitment (Figures 4E–4G) does not explain the de novo rhythmicity gained by a large group of genes in HFD (Figure 2B). Notably, with the exception of the group of genes whose oscillation is lost under HFD, the group of newly oscillating genes is the largest, more than doubling the number of genes that showed phase advancement as a result of the HFD.

Transcription factor motif analysis by MotifMap (Daily et al., 2011; Xie et al., 2009) was performed on a region located 10 kb upstream and 3 kb downstream of the transcriptional start sites to determine what transcriptional pathways might be most heavily affected by the HFD. Using a Bayesian branch length score of 1 or greater, E boxes were significantly enriched in genes oscillating only under NC, as well as in genes oscillating under both NC and HFD conditions. On the contrary, no enrichment for E boxes was observed in the group of genes oscillating exclusively in HFD condition. Analysis of the frequency of specific transcription factor binding sites in the promoters of genes whose oscillation was induced by HFD revealed that HFD promotes the use of additional transcriptional pathways to reprogram the hepatic transcriptome. One of the most represented transcription factors in the newly oscillating group of genes was PPARγ. Several other transcription factors oscillated in HF only, which included SREBP-1 (*Srebf*), CREB1, and SRF (Table S3). PPARγ and SREBP1 were identified as having one or more target sites in 322 and 91 genes, respectively (Figure 5A). In line with the idea of increased PPARγ-mediated gene expression under HFD, metabolomics analysis revealed that PPARγ ligands were elevated in livers of HFD-fed animals, specifically 13-HODE, 15-HETE, linolenate, and arachidonate (http://circadiomics.igb.uci.edu/ and Figure S4). PPARγ is a nuclear receptor involved in glucose and lipid metabolism (Fajas et al.,

Figure 3. A HFD Disrupts Circadian Organization between the Transcriptome and Metabolome

(A) Heat map showing the relationships between all pairs of metabolites and enzymes in KEGG. (Note: "flat" is a subset of "not," where the maximum abundance does not exceed the minimum by 20%.) Circled are the numbers referring to the five most common relationships.

(B) Related enzyme transcripts and metabolites ("edges") that follow a particular temporal profile.

(C) Metabolites and related transcripts within the SAM node that gain oscillation in HF.

(D) Oscillatory abundance of SAM, SAH, and their related enzymes *Ehmt2* and *Ahcyl2* only in HF.

Error bars, SEM.

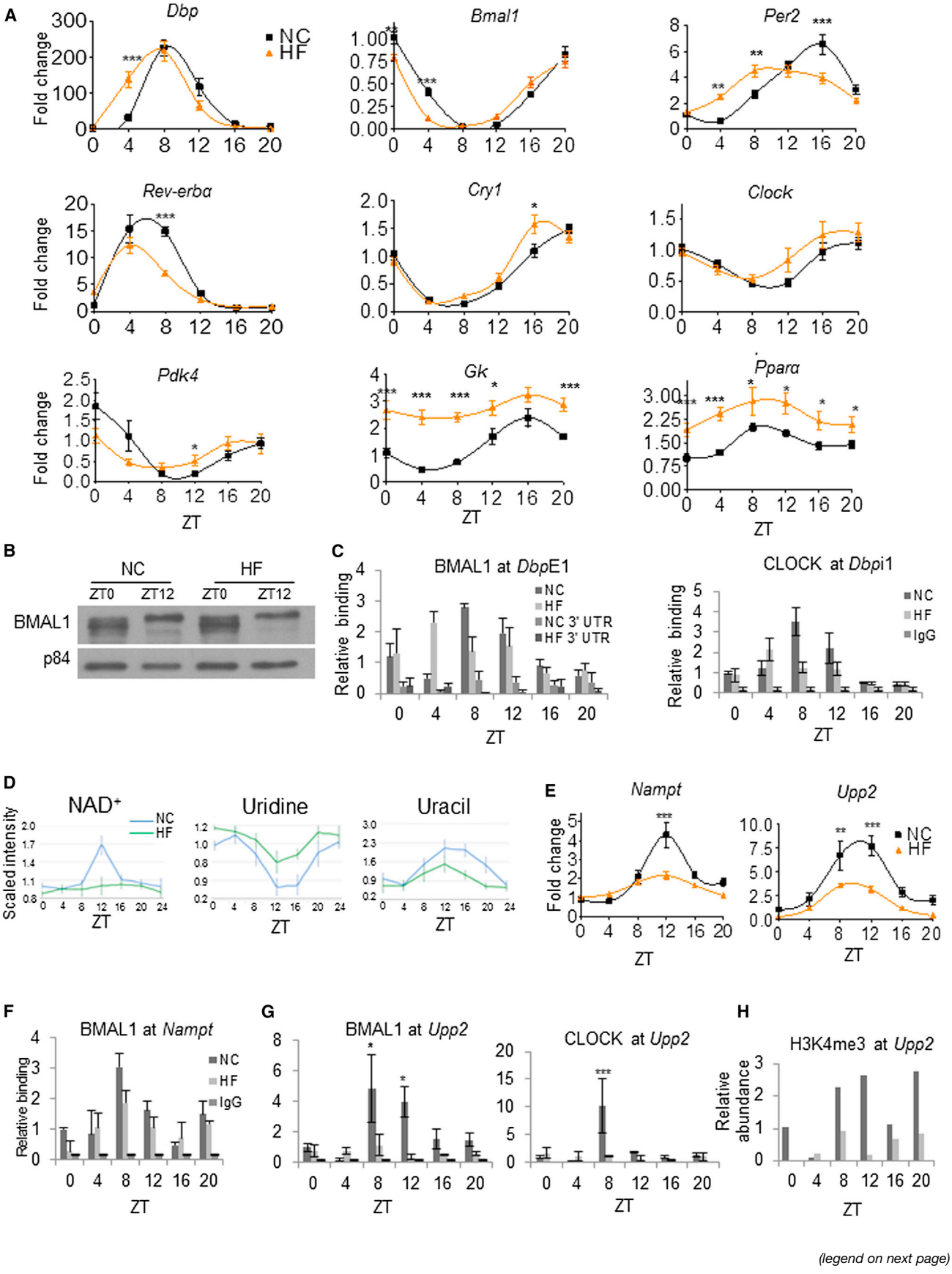

(legend on next page)

2001; Perreault et al., 2010) and has been described as a nutrient sensor in metabolic tissues (Spiegelman, 1998; Tontonoz and Spiegelman, 2008). PPARγ expression is induced in response to HFD (Vidal-Puig et al., 1996) and during the development of diet-induced fatty liver disease (Inoue et al., 2005). We found that *PPARγ* expression was robustly oscillatory in the liver of HFD-fed animals, with a peak at ZT12 (Figure 5B). Whereas the levels of total PPARγ protein were elevated, but not circadian, in HFD-fed mice (Figure 5C), nuclear PPARγ showed a significant circadian oscillation (Figure 5C), with a robust peak in expression at ZT12 (Figure 5D). Levels of PPARγ in NC-fed mice had no variation (Figures 5C and 5D). Importantly, chromatin-bound PPARγ displayed a robust change at different zeitgebers only in HFD-fed mice (Figure 5C). Expression of nocturnin (NOC), which has been implicated in PPARγ nuclear translocation in adipocytes (Kawai et al., 2010), was phase advanced under HFD but showed similar amplitude under both diets (Figure S4B).

We next analyzed the expression of several known PPARγ target genes. Cell-death-inducing DFFA-like effector c (*Cidec*, also known as fat-specific protein 27-*Fsp27*) is substantially elevated in the livers of the obese *ob/ob* mice (Matsusue et al., 2008). *Cidec* expression is not considered to be circadian under normal conditions but became robustly oscillatory under HFD (Figure 5E), corresponding with a circadian change in H3K4me3 at its promoter (Figure 5F). We validated the role of PPARγ by injecting GW9662, a specific PPARγ antagonist, into HFD-fed animals. GW9662 blocks PPARγ activity while not affecting its binding to DNA (Leesnitzer et al., 2002). While the circadian fluctuation in PPARγ in the chromatin fraction was unaltered, GW9662 produced a decrease in PPARγ-induced *Cidec* expression at the peak (Figure 5G). Furthermore, we found that PPARγ occupied the *Cidec* promoter in a circadian manner only in HFD-fed animals (Figure 5H). We analyzed another known PPARγ target, pyruvate carboxylase (*Pcx*), an enzyme that converts pyruvate to oxaloacetate and is an important regulator of hepatic gluconeogenesis (Jitrapakdee et al., 2006). Liver- and adipose-specific inhibition of *Pcx* produces a reduction in plasma glucose, adiposity, plasma lipid concentrations, and hepatic steatosis in HFD-fed animals (Kumashiro et al., 2013). *Pcx* expression was significantly elevated and rhythmic in livers of HFD-fed mice (Figure 5I, left), and PPARγ occupied the *Pcx* promoter in a circadian manner only in HFD conditions (Figure 5J). Thus, the transcriptional reprogramming induced by HFD relies on changes in the presence and pattern of oscillation and chromatin recruitment of PPARγ.

HFD-Induced Remodeling of the Clock Is Dissociable from Obesity

Animals fed a HFD for 10 weeks become obese (West et al., 1992; Figure S1A). To discern whether clock reprogramming depends on the development of obesity rather than the HFD content, we fed mice a HFD for only 3 days (Figure S5A) and then analyzed the metabolome. Considering only metabolites that showed consistent circadian profiles in NC between the 10 week group and the 3 day groups at the zeitgeber times chosen (this comparison revealed 87.5% consistency between experiments), 131 metabolites showed a diet effect, whereas 80 showed a time effect (Figure 6A and Table S4). We used NAD^+, uridine, and uracil as metabolic markers as they were highly susceptible to 10 weeks of HFD (Figure 4). Notably, the abundance and oscillation of uracil and uridine was greatly reduced in amplitude, and the circadian oscillation of NAD^+ was abolished within 3 days of HFD (Figure 6B). Next, we determined the impact of the 3 day feeding paradigm on transcription. *Bmal1* transcript and protein levels were unchanged by the 3 days of HFD, paralleling the scenario of the 10 week HFD (compare Figures 6C, 6D, 4A, and 4B). However, the amplitude of *Upp2* and *Nampt* oscillation was already reduced after 3 days of HFD, as was the expression of *Dbp* at ZT12, a reflection of the phase shift observed in the 10 weeks HFD analysis (Figure 6E). Finally, PPARγ targets gained rhythmicity after acute HFD feeding as illustrated by *Cidec* expression (Figure 6E).

In addition to the NC diet, a second low-fat diet (D12450B, Research Diets) was used to confirm that observed changes at 3 days were not simply due to variation in carbohydrate composition. Results were similar to NC-fed animals (data not shown), underscoring the deleterious nature of HFD on the circadian clock. Chromatin immunoprecipitation experiments revealed that the occupancy of CLOCK and BMAL1 was reduced at their target sites on *Upp2* and *Dbp* at ZT12 (Figure 6F), as was the H3K4me3 mark at these promoters (Figure 6G). Thus, a short 3 day exposure to HFD initiates the reprogramming of the circadian clock.

HFD-Induced Circadian Remodeling Is Reversible

To determine whether the transcriptional state of HFD-fed mice is reversible, we fed a group of animals a HFD for 10 weeks followed by 2 weeks of NC feeding. Although animals lost some

Figure 4. A HFD Disrupts Uridine and NAD^+ Metabolism by Impairing CLOCK:BMAL1 Recruitment

(A) Validation of microarray data by qPCR of clock and metabolic genes in NC and HF livers (n = 10 biological replicates per ZT per feeding condition).

(B) BMAL1 protein in nuclear lysates of NC and HF livers (Figure S4).

(C) BMAL1 and CLOCK occupancy at the E1 and I1 positions of the *Dbp* promoter as well as its 3′ UTR (CLOCK at *Dbp*i1- ****-time; **-interaction).

(D) Oscillation of NAD^+, uridine, and uracil in NC (blue) and HF (green) (n = 5).

(E) Oscillation of *Nampt* and *Upp2* mRNA in NC (black squares) and HF (orange triangles) livers (n = 10, *Upp2*: ***-time, ***-diet, ***-interaction; *Nampt* ****-time, ****-diet, ****- interaction; two-way ANOVA).

(F) BMAL1 occupancy at the promoter of *Nampt*.

(G) Relative binding of BMAL1 and CLOCK at the promoter of *Upp2*. (BMAL1 binding: ** - diet, *-time, * - interaction; CLOCK binding-* - time, *- interaction; two-way ANOVA, n = 4).

(H) H3K4me3 at the promoter of *Upp2* in NC and HF-fed animals (*-diet; two-way ANOVA, n = 2 biological replicates). *$p < 0.05$, **$p < 0.01$, ***$p < 0.001$, and ****$p < 0.0001$, Bonferroni posttests. Error bars, SEM.

See also Figure S3.

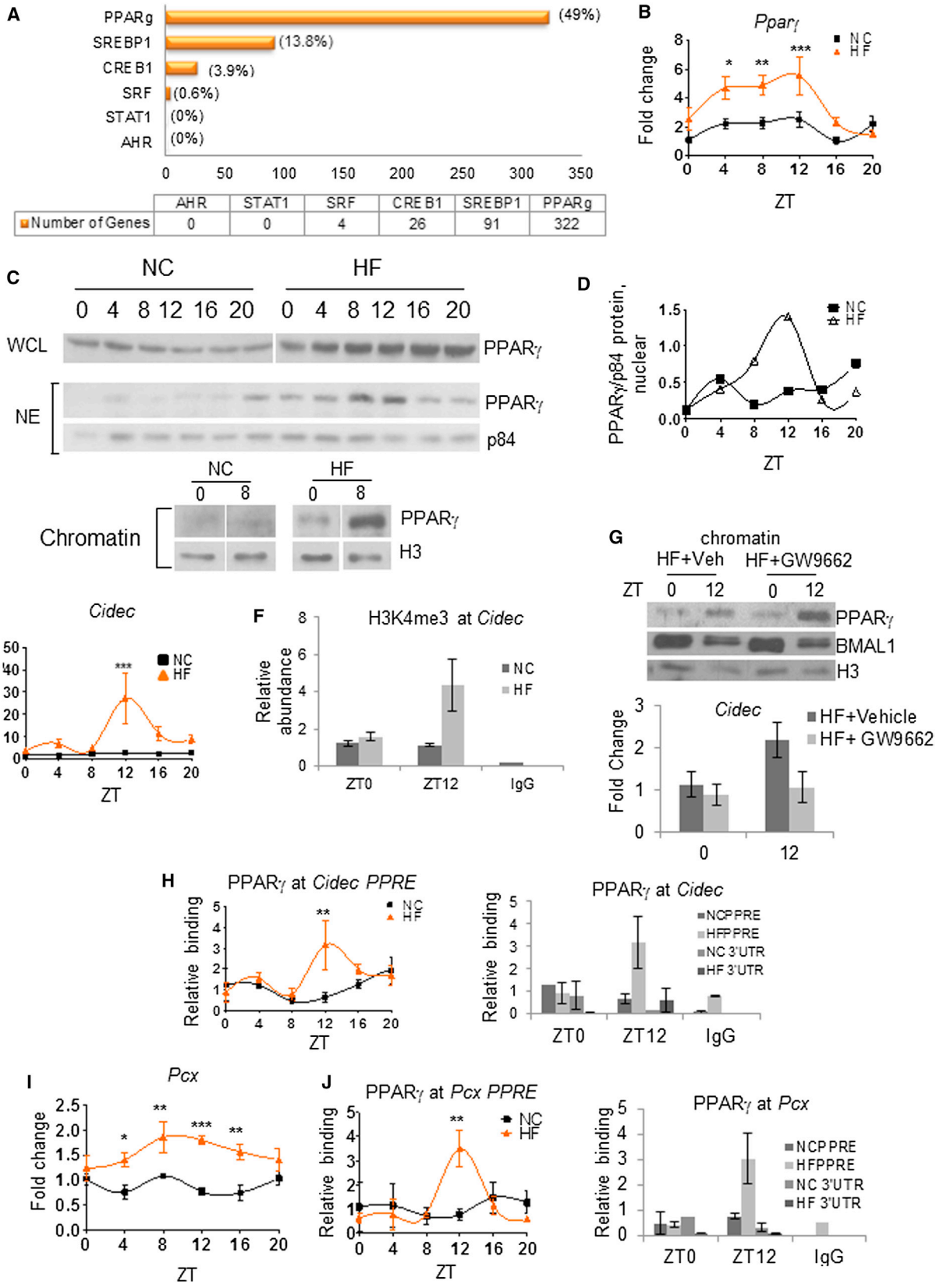

(legend on next page)

weight during the 2 week NC period, they remained significantly overweight relative to normal chow (Figure S5). Interestingly, after 2 weeks of NC feeding, circadian expression of *Upp2* and *Dbp* was restored (Figure 6H), as was *Nampt* (data not shown). Expression of the PPARγ target *Pcx* was not elevated relative to control livers at ZT12 (Figure 6H). Finally, BMAL1 occupancy at the *Upp2* and *Dbp* promoters at ZT12 was identical in both liver groups, revealing a restoration of circadian BMAL1 presence at target promoters after the HFD challenge was removed (Figure 6I). Thus, the HFD-induced transcriptional and epigenetic remodeling is reversible.

DISCUSSION

Metabolic and circadian processes are tightly linked, but the mechanisms by which altered nutrients influence the circadian clock have not been deciphered. We have explored the effects of nutrient challenge in the form of HFD on the circadian metabolome and transcriptome and found that HFD induces transcriptional reprogramming within the clock that reorganizes the relationships between the circadian transcriptome and the metabolome. We have unraveled at least three mechanisms by which this reprograming occurs: (1) loss of oscillation of a large number of normally oscillating genes; (2) a phase advance of an additional subset of oscillating transcripts; and (3) a massive induction of de novo oscillating gene transcripts.

We have demonstrated that HFD-induced changes in the circadian clock implicate a reprogramming of the transcriptional system that relies on at least two key mechanisms. The first mechanism is the lack of proper CLOCK:BMAL1 chromatin recruitment to genes that would normally be considered as clock controlled. This results in a decrease or abrogation of oscillation in transcription. The second, illustrated by the de novo oscillations in transcriptional networks otherwise considered arrhythmic, relies in large part on the robust, circadian accumulation in the nucleus and on chromatin of the transcription factor PPARγ (Figure 7). Although we predict that other transcriptional pathways would contribute to clock reprogramming, including SREBP1 (Figure 5A), the role of PPARγ appears prominent. This nuclear receptor has been linked to circadian control during adipogenesis and osteogenesis (Kawai et al., 2010), whereas its role in the liver clock is not fully understood (Green et al., 2007). We determine that PPARγ circadian function in HFD-fed mice relies on a clock-controlled nuclear translocation of the protein and rhythmic chromatin recruitment to target genes (Figures 5C, 5G, and 5I).

In contrast to the PPARγ scenario, HFD does not affect CLOCK:BMAL1 nuclear translocation but impedes their specific chromatin recruitment (Figure 4). We speculate that additional regulatory pathways are implicated that might interplay with the ones described here. In conclusion, the remarkable induction of de novo oscillation in both metabolites and transcripts under HFD indicates that a diet high in fat has previously unsuspected, potent, and pleiotropic effects on the circadian clock. Furthermore, the rapid influence of the diet on the clock (as demonstrated by the 3 day HFD experiment; Figure 6D) reveals that this type of nutritional challenge—and not merely the development of diet-associated complications such as obesity—is capable of remodeling the clock. Further work will elucidate how the molecular composition of CLOCK:BMAL1 and PPARγ chromatin complexes may be influenced by nutritional challenges, possibly leading to modulation of enzymatic activities of specific coregulators and modifiers.

An intriguing concept that may be derived from our study relates to the potential of specific genes to be circadian or not. Indeed, the transcriptional remodeling in the HFD raises the hypothesis that, given the "right" molecular environment, an extended array of transcripts and metabolites can oscillate. We speculate that this may be achieved through the coordinated harmonics of energy balance, transcriptional control, and epigenetic state. In summary, nutrients have powerful effects on the cellular clock, revealing its intrinsic plasticity. These effects consist not only of the abrogation of pre-existing rhythms but the genesis of rhythms where they do not normally exist. This induction is rapid and does not require the onset of obesity, and it is also reversible. The reversible nature of these effects gives hope for novel nutritional and pharmaceutical strategies.

EXPERIMENTAL PROCEDURES

Mice

Age-matched, male C57BL/6J mice (JAX, 00064) were maintained on a 12 hr light/12 hr dark cycle. Animal care and use was in accordance with guidelines of the Institutional Animal Care and Use Committee at the University of California at Irvine.

Feeding

At 6 weeks of age, animals were placed on a normal chow diet (Prolab RMH 2500), or a HFD (60% kcal from fat, Research Diets, D12492) for 10 weeks. Additional 3 day feeding experiments included Prolab RMH 25040

Figure 5. HFD-Induced Transcriptional Reprogramming of the Hepatic Clock

(A) Number of newly oscillating genes in HF livers containing PPARγ, SREBP1, CREB1, SRF, STAT1, or AHR sites.

(B) *Pparγ* mRNA in NC (black squares) and HF (orange triangles) livers (n = 5).

(C) PPARγ abundance in whole-cell lysates (WCL), nuclear extracts (NE), and chromatin extracts (Chromatin) in animals fed NC or HF diet for 10 weeks (each lane consists of PPARγ protein from three pooled livers).

(D) Quantification of nuclear PPARγ protein normalized to the nuclear protein p84. Units are expressed as relative optical density.

(E) Circadian abundance of *Cidec* mRNA.

(F) Circadian change in H3K4me3 at the *Cidec* promoter.

(G) PPARγ chromatin recruitment and *Cidec* expression relative to *18S* and *Pparγ* in livers of animals on HF treated with PPARγ antagonist, GW9662, or vehicle.

(H) Rhythmic PPARγ recruitment to the promoter of *Cidec*, but not its 3′ UTR.

(I) *Pcx* mRNA in NC- and HF-fed animals.

(I and J) Binding of PPARγ to the promoter PPARγ response elements (PPRE) and 3′ UTR at the *Pcx* gene. Error bars, SEM.

See also Figure S4.

A

Statistical Comparisons of 321 Metabolites	
Two Way ANOVA	Biochemicals with P<0.05
Diet Effect	131
Time Effect	80
Diet: Time Interaction	17

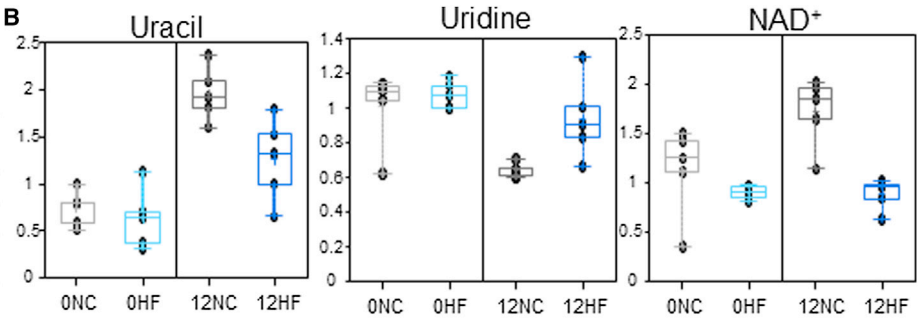

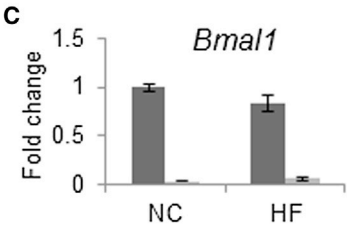

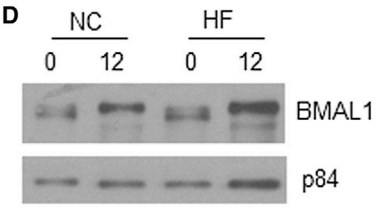

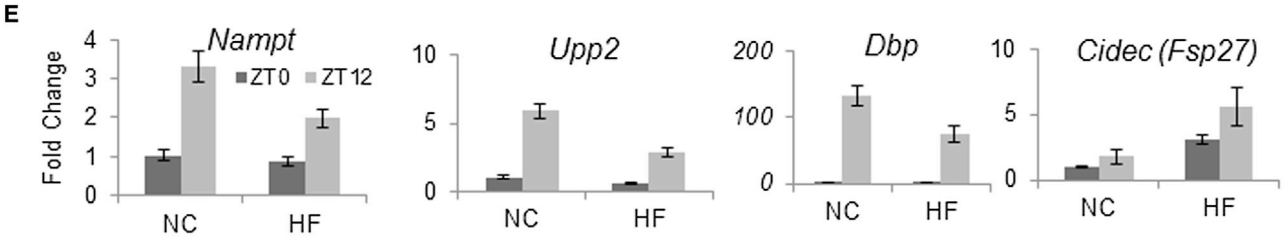

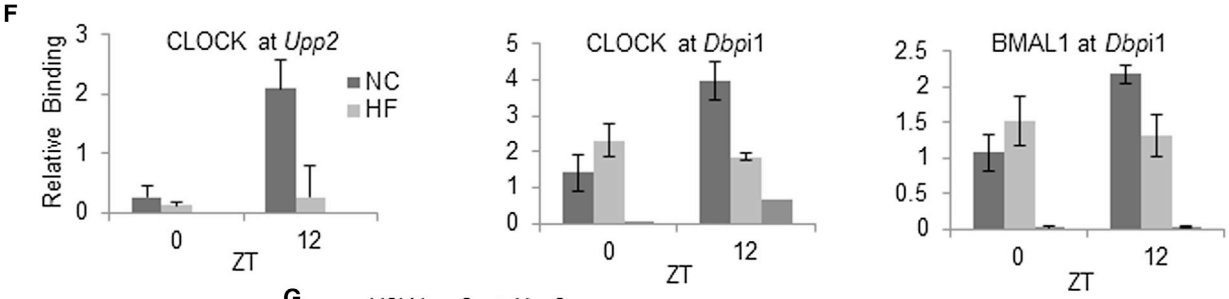

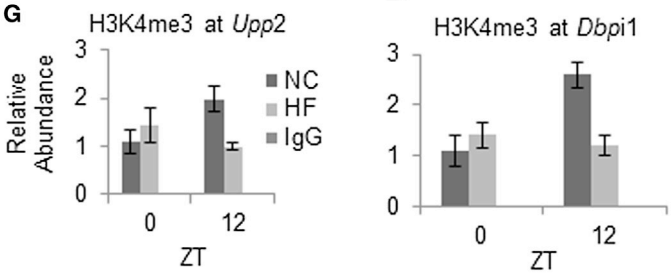

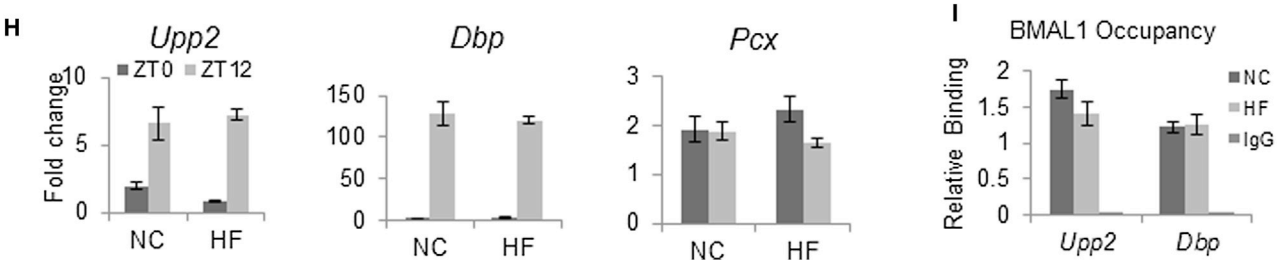

(legend on next page)

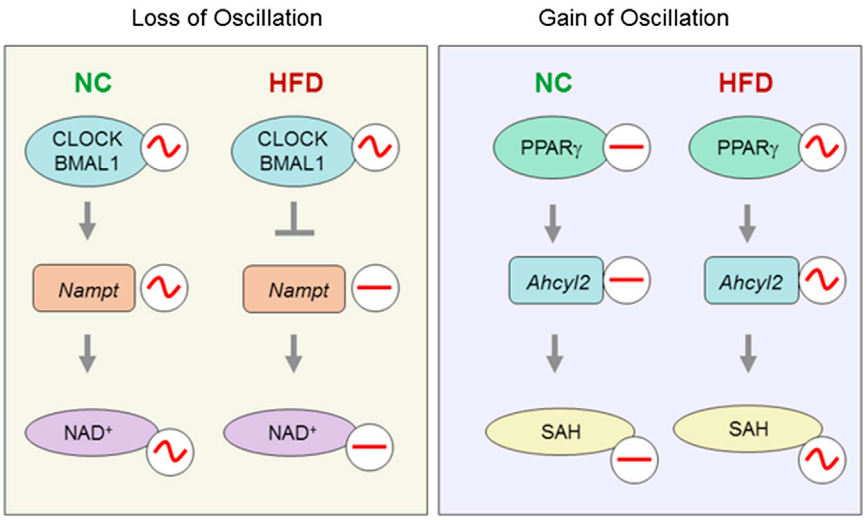

Figure 7. Nutrient Insult Restructures the Hepatic Circadian Clock

A HFD both blocks oscillations within the previously existing clock system and triggers new oscillations where they previously did not exist.

(12.1% kcal from fat), RD D12492 (10% kcal from fat), and RD D12450B (60% kcal from fat) diets. To maintain consistency with prior metabolomic experiments, metabolomics was performed on livers from animals on the Prolab RMH 25040 and RD D12450B diets. Body weight was measured weekly. Animals were separated into individual cages 1 week prior to sacrifice.

Microarray Analysis

Microarrays were performed at the UCI Genomics High-Throughput Facility, University of California, Irvine (see Extended Experimental Procedures). Data sets can be found in the NCBI Gene Expression Omnibus (GEO), GSE52333.

Gene Annotation

Gene annotation was performed using Genecodis (Carmona-Saez et al., 2007; Nogales-Cadenas et al., 2009).

MotifMap Analysis

MotifMap is a comprehensive database of putative regulatory transcription factor binding sites that is described in Daily et al. (2011) and Xie et al. (2009). See also Extended Experimental Procedures.

ChIP

ChIP experiments were performed as previously described (Eckel-Mahan et al., 2012) (see also Extended Experimental Procedures).

Western Blot Analysis and Quantification

Generally, 3–15 μg protein of liver nuclear extracts was loaded on 8% polyacrylamide gels. Antibodies include those listed for ChIP as well as p84 (5E10, GeneTex, 1:3,000). BMAL1 was used at a concentration of 1:2,000, and all other primary antibodies were used at a concentration of 1:1,000.

GW9662 Administration

GW9662 (Cayman Chemical) was prepared as previously described (Sos et al., 2011) and administered at a dose of 4 mg/kg (see Extended Experimental Procedures).

Statistics

Data represent mean ± SEM of experiments. Experiments with two variables were analyzed by two-way ANOVA using Bonferroni posttests (Prism 5.0). Mann-Whitney U tests were used to analyze two independent samples when $n \leq 10$. For analysis of rhythmic metabolites and transcripts, the nonparametric test JTK_CYCLE was used incorporating a window of 20–28 hr for the determination of circadian periodicity as described in Eckel-Mahan et al. (2012) and Hughes et al. (2010) (Tables S2 and S3). For transcript annotation and oscillation analysis, $p < 0.01$ was considered significant. For metabolite analysis, $p < 0.05$ was considered significant, and for metabolite:transcript relationship evaluation only, p values extending to 0.1 were allowed for metabolite oscillations exclusively.

ACCESSION NUMBERS

The GEO accession number for the microarray data set reported in this paper is GSE52333.

SUPPLEMENTAL INFORMATION

Supplemental Information includes Extended Experimental Procedures, five figures, and four tables and can be found with this article online at http://dx.doi.org/10.1016/j.cell.2013.11.034.

ACKNOWLEDGMENTS

We thank members of the Sassone-Corsi laboratory for constructive comments. We would also like to thank Melanie Oakes, Seung-Ah Chung, and Valentina Ciobanu at the UCI Genomics High-Throughput Facility at the University of California, Irvine. We are grateful to Janice Jones, Jeff Buckthal, Robert Eckel, Hong Wang, Selma Masri, and Jennifer Mondok for helpful comments regarding the data or for technical assistance. Monetary support includes NIH/NRSA F32 DK083881 (K.L.E.-M.), NIH grants GM081634 and AG033888

Figure 6. Acute Administration of a HFD, and Not the Presence of Obesity, Is Sufficient to Reorganize the Hepatic Circadian Clock

(A) The number of hepatic metabolites affected by acute (3 day) HFD feeding.
(B) Relative abundance of metabolites uracil, uridine, and NAD^+ after acute HF diet. (0NC = ZT0, normal chow; 0HF = ZT0, HF diet).
(C) *Bmal1* mRNA after 3 days on NC or HF diets (***-time, n = 5).
(D) Western blot of nuclear BMAL1 and p84 proteins.
(E) BMAL1 targets (*Nampt*, *Upp2*, and *Dbp*) and PPARγ target (*Cidec*) after acute HF feeding. (*Nampt*, ***-time; *-diet; *Upp2*, ***-time; ***-diet, **-time/diet interaction; *Dbp*, ***-time; *Cidec*, *-time; n = 5.)
(F) CLOCK and BMAL1 occupancy at the *Upp2* and *Dbp* promoter after 3 day feeding. Clock occupancy, *Upp2*: **-time; **-diet *- interaction; CLOCK occupancy, Dbpi1: *-time; **- interaction; BMAL1 occupancy Dbpi1: *- interaction.
(G) H3K4me3 marks at the *Upp2* and *Dbp* promoters after 3 day feeding. H3K4me3 at Dbpi1: *-time; **- interaction, n = 4.)
(H) Hepatic expression of *Upp2*, *Dbp*, and *Pcx* in animals removed from the HFD for 2 weeks (*Upp2*: ***-time, *Dbp*; ***-time, n = 5).
(I) BMAL1 occupancy at ZT12 at the promoters of *Upp2* and *Dbp* in NC mice and mice withdrawn from the HFD for 2 weeks. Error bars, SEM; ***$p < 0.001$, **$p < 0.01$, and *$p < 0.05$.
See also Figure S5 and Table S4.

(P.S.-C.), Merieux Research Grant, and Sirtris Pharmaceuticals SP-48984 (P.S.-C.). The work of V.R.P., N.J.C., and P.B. is supported by NSF IIS-0513376, NIH LM010235, and NIH-NLM T15 LM07443 to P.B.

Received: August 5, 2013
Revised: October 16, 2013
Accepted: November 21, 2013
Published: December 19, 2013

REFERENCES

Antunes, Lda.C., Jornada, M.N., Ramalho, L., and Hidalgo, M.P. (2010). Correlation of shift work and waist circumference, body mass index, chronotype and depressive symptoms. Arq. Bras. Endocrinol. Metabol. *54*, 652–656.

Arble, D.M., Bass, J., Laposky, A.D., Vitaterna, M.H., and Turek, F.W. (2009). Circadian timing of food intake contributes to weight gain. Obesity (Silver Spring) *17*, 2100–2102.

Bray, M.S., and Young, M.E. (2009). The role of cell-specific circadian clocks in metabolism and disease. Obes. Rev. *10*, 6–13.

Carmona-Saez, P., Chagoyen, M., Tirado, F., Carazo, J.M., and Pascual-Montano, A. (2007). GENECODIS: a web-based tool for finding significant concurrent annotations in gene lists. Genome Biol. *8*, R3.

Daily, K., Patel, V.R., Rigor, P., Xie, X., and Baldi, P. (2011). MotifMap: integrative genome-wide maps of regulatory motif sites for model species. BMC Bioinformatics *12*, 495.

Dallmann, R., Viola, A.U., Tarokh, L., Cajochen, C., and Brown, S.A. (2012). The human circadian metabolome. Proc. Natl. Acad. Sci. USA *109*, 2625–2629.

Damiola, F., Le Minh, N., Preitner, N., Kornmann, B., Fleury-Olela, F., and Schibler, U. (2000). Restricted feeding uncouples circadian oscillators in peripheral tissues from the central pacemaker in the suprachiasmatic nucleus. Genes Dev. *14*, 2950–2961.

Das, U.N., and Rao, A.A. (2007). Gene expression profile in obesity and type 2 diabetes mellitus. Lipids Health Dis. *6*, 35.

Dibner, C., Schibler, U., and Albrecht, U. (2010). The mammalian circadian timing system: organization and coordination of central and peripheral clocks. Annu. Rev. Physiol. *72*, 517–549.

Doi, M., Takahashi, Y., Komatsu, R., Yamazaki, F., Yamada, H., Haraguchi, S., Emoto, N., Okuno, Y., Tsujimoto, G., Kanematsu, A., et al. (2010). Salt-sensitive hypertension in circadian clock-deficient Cry-null mice involves dysregulated adrenal Hsd3b6. Nat. Med. *16*, 67–74.

Drake, C.L., Roehrs, T., Richardson, G., Walsh, J.K., and Roth, T. (2004). Shift work sleep disorder: prevalence and consequences beyond that of symptomatic day workers. Sleep *27*, 1453–1462.

Eckel-Mahan, K.L., Patel, V.R., Mohney, R.P., Vignola, K.S., Baldi, P., and Sassone-Corsi, P. (2012). Coordination of the transcriptome and metabolome by the circadian clock. Proc. Natl. Acad. Sci. USA *109*, 5541–5546.

Evans, A.M., DeHaven, C.D., Barrett, T., Mitchell, M., and Milgram, E. (2009). Integrated, nontargeted ultrahigh performance liquid chromatography/electrospray ionization tandem mass spectrometry platform for the identification and relative quantification of the small-molecule complement of biological systems. Anal. Chem. *81*, 6656–6667.

Fajas, L., Debril, M.B., and Auwerx, J. (2001). PPAR gamma: an essential role in metabolic control. Nutr. Metab. Cardiovasc. Dis. *11*, 64–69.

Feng, D., and Lazar, M.A. (2012). Clocks, metabolism, and the epigenome. Mol. Cell *47*, 158–167.

Fonken, L.K., Workman, J.L., Walton, J.C., Weil, Z.M., Morris, J.S., Haim, A., and Nelson, R.J. (2010). Light at night increases body mass by shifting the time of food intake. Proc. Natl. Acad. Sci. USA *107*, 18664–18669.

Froy, O. (2010). Metabolism and circadian rhythms—implications for obesity. Endocr. Rev. *31*, 1–24.

Gerstner, J.R., Lyons, L.C., Wright, K.P., Jr., Loh, D.H., Rawashdeh, O., Eckel-Mahan, K.L., and Roman, G.W. (2009). Cycling behavior and memory formation. J. Neurosci. *29*, 12824–12830.

Green, C.B., Douris, N., Kojima, S., Strayer, C.A., Fogerty, J., Lourim, D., Keller, S.R., and Besharse, J.C. (2007). Loss of Nocturnin, a circadian deadenylase, confers resistance to hepatic steatosis and diet-induced obesity. Proc. Natl. Acad. Sci. USA *104*, 9888–9893.

Hastings, M.H., Maywood, E.S., and Reddy, A.B. (2008). Two decades of circadian time. J. Neuroendocrinol. *20*, 812–819.

Hatanaka, F., Matsubara, C., Myung, J., Yoritaka, T., Kamimura, N., Tsutsumi, S., Kanai, A., Suzuki, Y., Sassone-Corsi, P., Aburatani, H., et al. (2010). Genome-wide profiling of the core clock protein BMAL1 targets reveals a strict relationship with metabolism. Mol. Cell. Biol. *30*, 5636–5648.

Hatori, M., Vollmers, C., Zarrinpar, A., DiTacchio, L., Bushong, E.A., Gill, S., Leblanc, M., Chaix, A., Joens, M., Fitzpatrick, J.A., et al. (2012). Time-restricted feeding without reducing caloric intake prevents metabolic diseases in mice fed a high-fat diet. Cell Metab. *15*, 848–860.

Hughes, M.E., DiTacchio, L., Hayes, K.R., Vollmers, C., Pulivarthy, S., Baggs, J.E., Panda, S., and Hogenesch, J.B. (2009). Harmonics of circadian gene transcription in mammals. PLoS Genet. *5*, e1000442.

Hughes, M.E., Hogenesch, J.B., and Kornacker, K. (2010). JTK_CYCLE: an efficient nonparametric algorithm for detecting rhythmic components in genome-scale data sets. J. Biol. Rhythms *25*, 372–380.

Inoue, M., Ohtake, T., Motomura, W., Takahashi, N., Hosoki, Y., Miyoshi, S., Suzuki, Y., Saito, H., Kohgo, Y., and Okumura, T. (2005). Increased expression of PPARgamma in high fat diet-induced liver steatosis in mice. Biochem. Biophys. Res. Commun. *336*, 215–222.

Itoh, N., Sakaue, S., Nakagawa, H., Kurogochi, M., Ohira, H., Deguchi, K., Nishimura, S., and Nishimura, M. (2007). Analysis of N-glycan in serum glycoproteins from db/db mice and humans with type 2 diabetes. Am. J. Physiol. Endocrinol. Metab. *293*, E1069–E1077.

Jitrapakdee, S., Vidal-Puig, A., and Wallace, J.C. (2006). Anaplerotic roles of pyruvate carboxylase in mammalian tissues. Cell. Mol. Life Sci. *63*, 843–854.

Kasukawa, T., Sugimoto, M., Hida, A., Minami, Y., Mori, M., Honma, S., Honma, K., Mishima, K., Soga, T., and Ueda, H.R. (2012). Human blood metabolite timetable indicates internal body time. Proc. Natl. Acad. Sci. USA *109*, 15036–15041.

Katada, S., and Sassone-Corsi, P. (2010). The histone methyltransferase MLL1 permits the oscillation of circadian gene expression. Nat. Struct. Mol. Biol. *17*, 1414–1421.

Kawai, M., Green, C.B., Lecka-Czernik, B., Douris, N., Gilbert, M.R., Kojima, S., Ackert-Bicknell, C., Garg, N., Horowitz, M.C., Adamo, M.L., et al. (2010). A circadian-regulated gene, Nocturnin, promotes adipogenesis by stimulating PPAR-gamma nuclear translocation. Proc. Natl. Acad. Sci. USA *107*, 10508–10513.

Knutsson, A. (2003). Health disorders of shift workers. Occup. Med. (Lond.) *53*, 103–108.

Ko, C.H., and Takahashi, J.S. (2006). Molecular components of the mammalian circadian clock. Hum. Mol. Genet. *15* (Spec No 2), R271–R277.

Kohsaka, A., Laposky, A.D., Ramsey, K.M., Estrada, C., Joshu, C., Kobayashi, Y., Turek, F.W., and Bass, J. (2007). High-fat diet disrupts behavioral and molecular circadian rhythms in mice. Cell Metab. *6*, 414–421.

Koike, N., Yoo, S.H., Huang, H.C., Kumar, V., Lee, C., Kim, T.K., and Takahashi, J.S. (2012). Transcriptional architecture and chromatin landscape of the core circadian clock in mammals. Science *338*, 349–354.

Kondratov, R.V., Chernov, M.V., Kondratova, A.A., Gorbacheva, V.Y., Gudkov, A.V., and Antoch, M.P. (2003). BMAL1-dependent circadian oscillation of nuclear CLOCK: posttranslational events induced by dimerization of transcriptional activators of the mammalian clock system. Genes Dev. *17*, 1921–1932.

Kondratov, R.V., Kondratova, A.A., Gorbacheva, V.Y., Vykhovanets, O.V., and Antoch, M.P. (2006). Early aging and age-related pathologies in mice deficient in BMAL1, the core componentof the circadian clock. Genes Dev. *20*, 1868–1873.

Kumashiro, N., Beddow, S.A., Vatner, D.F., Majumdar, S.K., Cantley, J.L., Guebre-Egziabher, F., Fat, I., Guigni, B., Jurczak, M.J., Birkenfeld, A.L.,

Kahn, M., et al. (2013). Targeting pyruvate carboxylase reduces gluconeogenesis and adiposity and improves insulin resistance. Diabetes *62*, 2183–2194.

Lamia, K.A., Storch, K.F., and Weitz, C.J. (2008). Physiological significance of a peripheral tissue circadian clock. Proc. Natl. Acad. Sci. USA *105*, 15172–15177.

Lee, J., Kim, M.S., Li, R., Liu, V.Y., Fu, L., Moore, D.D., Ma, K., and Yechoor, V.K. (2011). Loss of Bmal1 leads to uncoupling and impaired glucose-stimulated insulin secretion in beta-cells. Islets *3*, 381–388.

Leesnitzer, L.M., Parks, D.J., Bledsoe, R.K., Cobb, J.E., Collins, J.L., Consler, T.G., Davis, R.G., Hull-Ryde, E.A., Lenhard, J.M., Patel, L., et al. (2002). Functional consequences of cysteine modification in the ligand binding sites of peroxisome proliferator activated receptors by GW9662. Biochemistry *41*, 6640–6650.

Marcheva, B., Ramsey, K.M., Buhr, E.D., Kobayashi, Y., Su, H., Ko, C.H., Ivanova, G., Omura, C., Mo, S., Vitaterna, M.H., et al. (2010). Disruption of the clock components CLOCK and BMAL1 leads to hypoinsulinaemia and diabetes. Nature *466*, 627–631.

Masri, S., Patel, V.R., Eckel-Mahan, K.L., Peleg, S., Forne, I., Ladurner, A.G., Baldi, P., Imhof, A., and Sassone-Corsi, P. (2013). Circadian acetylome reveals regulation of mitochondrial metabolic pathways. Proc. Natl. Acad. Sci. USA *110*, 3339–3344.

Matsusue, K., Kusakabe, T., Noguchi, T., Takiguchi, S., Suzuki, T., Yamano, S., and Gonzalez, F.J. (2008). Hepatic steatosis in leptin-deficient mice is promoted by the PPARgamma target gene Fsp27. Cell Metab. *7*, 302–311.

Menet, J.S., and Rosbash, M. (2011). When brain clocks lose track of time: cause or consequence of neuropsychiatric disorders. Curr. Opin. Neurobiol. *21*, 849–857.

Morf, J., Rey, G., Schneider, K., Stratmann, M., Fujita, J., Naef, F., and Schibler, U. (2012). Cold-inducible RNA-binding protein modulates circadian gene expression posttranscriptionally. Science *338*, 379–383.

Nakahata, Y., Sahar, S., Astarita, G., Kaluzova, M., and Sassone-Corsi, P. (2009). Circadian control of the NAD+ salvage pathway by CLOCK-SIRT1. Science *324*, 654–657.

Nogales-Cadenas, R., Carmona-Saez, P., Vazquez, M., Vicente, C., Yang, X., Tirado, F., Carazo, J.M., and Pascual-Montano, A. (2009). GeneCodis: interpreting gene lists through enrichment analysis and integration of diverse biological information. Nucleic Acids Res. *37*, W317–W322.

O'Neill, J.S., Maywood, E.S., Chesham, J.E., Takahashi, J.S., and Hastings, M.H. (2008). cAMP-dependent signaling as a core component of the mammalian circadian pacemaker. Science *320*, 949–953.

O'Neill, J.S., van Ooijen, G., Dixon, L.E., Troein, C., Corellou, F., Bouget, F.Y., Reddy, A.B., and Millar, A.J. (2011). Circadian rhythms persist without transcription in a eukaryote. Nature *469*, 554–558.

Patel, V.R., Eckel-Mahan, K., Sassone-Corsi, P., and Baldi, P. (2012). CircadiOmics: integrating circadian genomics, transcriptomics, proteomics and metabolomics. Nat. Methods *9*, 772–773.

Pendergast, J.S., Branecky, K.L., Yang, W., Ellacott, K.L., Niswender, K.D., and Yamazaki, S. (2013). High-fat diet acutely affects circadian organisation and eating behavior. Eur. J. Neurosci. *37*, 1350–1356.

Perreault, M., Will, S., Panza, D., Gareski, T., Harding, K., Kubasiak, D., Jalenak, M., Gartrell, K., Wang, S., Bollag, G., et al. (2010). Modulation of nutrient sensing nuclear hormone receptors promotes weight loss through appetite suppression in mice. Diabetes Obes. Metab. *12*, 234–245.

Ramsey, K.M., Yoshino, J., Brace, C.S., Abrassart, D., Kobayashi, Y., Marcheva, B., Hong, H.K., Chong, J.L., Buhr, E.D., Lee, C., et al. (2009). Circadian clock feedback cycle through NAMPT-mediated NAD+ biosynthesis. Science *324*, 651–654.

Rey, G., Cesbron, F., Rougemont, J., Reinke, H., Brunner, M., and Naef, F. (2011). Genome-wide and phase-specific DNA-binding rhythms of BMAL1 control circadian output functions in mouse liver. PLoS Biol. *9*, e1000595.

Ripperger, J.A., and Schibler, U. (2006). Rhythmic CLOCK-BMAL1 binding to multiple E-box motifs drives circadian Dbp transcription and chromatin transitions. Nat. Genet. *38*, 369–374.

Rodgers, J.T., Lerin, C., Haas, W., Gygi, S.P., Spiegelman, B.M., and Puigserver, P. (2005). Nutrient control of glucose homeostasis through a complex of PGC-1alpha and SIRT1. Nature *434*, 113–118.

Rudic, R.D., McNamara, P., Curtis, A.M., Boston, R.C., Panda, S., Hogenesch, J.B., and Fitzgerald, G.A. (2004). BMAL1 and CLOCK, two essential components of the circadian clock, are involved in glucose homeostasis. PLoS Biol. *2*, e377.

Sadacca, L.A., Lamia, K.A., deLemos, A.S., Blum, B., and Weitz, C.J. (2011). An intrinsic circadian clock of the pancreas is required for normal insulin release and glucose homeostasis in mice. Diabetologia *54*, 120–124.

Sahar, S., and Sassone-Corsi, P. (2012). Regulation of metabolism: the circadian clock dictates the time. Trends Endocrinol. Metab. *23*, 1–8.

Schibler, U., and Sassone-Corsi, P. (2002). A web of circadian pacemakers. Cell *111*, 919–922.

Sharifian, A., Farahani, S., Pasalar, P., Gharavi, M., and Aminian, O. (2005). Shift work as an oxidative stressor. J. Circadian Rhythms *3*, 15.

Shi, S.Q., Ansari, T.S., McGuinness, O.P., Wasserman, D.H., and Johnson, C.H. (2013). Circadian disruption leads to insulin resistance and obesity. Curr. Biol. *23*, 372–381.

Sos, B.C., Harris, C., Nordstrom, S.M., Tran, J.L., Balázs, M., Caplazi, P., Febbraio, M., Applegate, M.A., Wagner, K.U., and Weiss, E.J. (2011). Abrogation of growth hormone secretion rescues fatty liver in mice with hepatocyte-specific deletion of JAK2. J. Clin. Invest. *121*, 1412–1423.

Spiegelman, B.M. (1998). PPAR-gamma: adipogenic regulator and thiazolidinedione receptor. Diabetes *47*, 507–514.

Stokkan, K.A., Yamazaki, S., Tei, H., Sakaki, Y., and Menaker, M. (2001). Entrainment of the circadian clock in the liver by feeding. Science *291*, 490–493.

Suwazono, Y., Dochi, M., Sakata, K., Okubo, Y., Oishi, M., Tanaka, K., Kobayashi, E., Kido, T., and Nogawa, K. (2008). A longitudinal study on the effect of shift work on weight gain in male Japanese workers. Obesity (Silver Spring) *16*, 1887–1893.

Tontonoz, P., and Spiegelman, B.M. (2008). Fat and beyond: the diverse biology of PPARgamma. Annu. Rev. Biochem. *77*, 289–312.

Turek, F.W., Joshu, C., Kohsaka, A., Lin, E., Ivanova, G., McDearmon, E., Laposky, A., Losee-Olson, S., Easton, A., Jensen, D.R., et al. (2005). Obesity and metabolic syndrome in circadian Clock mutant mice. Science *308*, 1043–1045.

Vidal-Puig, A., Jimenez-Liñan, M., Lowell, B.B., Hamann, A., Hu, E., Spiegelman, B., Flier, J.S., and Moller, D.E. (1996). Regulation of PPAR gamma gene expression by nutrition and obesity in rodents. J. Clin. Invest. *97*, 2553–2561.

Vollmers, C., Gill, S., DiTacchio, L., Pulivarthy, S.R., Le, H.D., and Panda, S. (2009). Time of feeding and the intrinsic circadian clock drive rhythms in hepatic gene expression. Proc. Natl. Acad. Sci. USA *106*, 21453–21458.

West, D.B., Boozer, C.N., Moody, D.L., and Atkinson, R.L. (1992). Dietary obesity in nine inbred mouse strains. Am. J. Physiol. *262*, R1025–R1032.

Xie, X., Rigor, P., and Baldi, P. (2009). MotifMap: a human genome-wide map of candidate regulatory motif sites. Bioinformatics *25*, 167–174.

Yoo, S.H., Mohawk, J.A., Siepka, S.M., Shan, Y., Huh, S.K., Hong, H.K., Kornblum, I., Kumar, V., Koike, N., Xu, M., et al. (2013). Competing E3 ubiquitin ligases govern circadian periodicity by degradation of CRY in nucleus and cytoplasm. Cell *152*, 1091–1105.

Yoshino, J., Mills, K.F., Yoon, M.J., and Imai, S. (2011). Nicotinamide mononucleotide, a key NAD(+) intermediate, treats the pathophysiology of diet- and age-induced diabetes in mice. Cell Metab. *14*, 528–536.

Zhang, E.E., Liu, Y., Dentin, R., Pongsawakul, P.Y., Liu, A.C., Hirota, T., Nusinow, D.A., Sun, X., Landais, S., Kodama, Y., et al. (2010). Cryptochrome mediates circadian regulation of cAMP signaling and hepatic gluconeogenesis. Nat. Med. *16*, 1152–1156.